Lignin-incorporated nanogel serving as an antioxidant biomaterial for wound healing

Jia Xu[†], Jia Jia Xu[†], Qianyu Lin[‡], Lu Jiang[‡], Duoteng Zhang[†], Zibiao Li[‡], Bo Ma[†], Chengwu Zhang[†], Lin Li[†], Dan Kai*[‡], Hai-Dong Yu*[†§], Xian Jun Loh[‡]*

[†]Key Laboratory of Flexible Electronics (KLOFE) & Institute of Advanced Materials (IAM), Jiangsu National Synergetic Innovation Center for Advanced Materials (SICAM), Nanjing Tech University (Nanjing Tech), 30 South Puzhu Road, Nanjing, 211816, P.R. China

[‡]Institute of Materials Research and Engineering (IMRE), A*STAR, 2 Fusionopolis Way, #08-03 Innovis, Singapore 138634

[§]Frontiers Science Center for Flexible Electronics, Xi'an Institute of Flexible Electronics (IFE) and Xi'an Institute of Biomedical Materials & Engineering, Northwestern Polytechnical University, 127 West Youyi Road, Xi'an 710072, P. R. China

ABSTRACT

Oxidative phosphorylation is an important biological process of the body to produce energy, during which oxygen free radicals are generated as by product. Excessive oxygen free radicals cause cell death and reduce the rate of tissue regeneration and healing in wound. Lignin is a natural antioxidant derived from plants, but its biomedical application is restricted due to the uncertain biocompatibility. In this work, we developed a lignin-incorporated nanogel and explored its

application for wound healing. Lignin was extracted from coconut husks and was determined to have strong antioxidant activity (IC_{50} = 25.7 ppm). Various amounts of lignin were incorporated into thermo-responsive nanogels, which were produced from polyurethane copolymers of polyethylene glycol (PEG), polypropylene glycol (PPG), and polydimethylsiloxane (PDMS). It was shown that the addition of lignin had minimal effects on the gelation and rheological properties of the nanogel but slightly increased the critical micelle concentration (CMC) of poly (PEG/PPG/PDMS urethane) copolymer from 3.38×10^{-4} g·mL^{-1} to 4.61×10^{-4} g·mL^{-1}. The lignin-incorporated nanogels did not display detectable cytotoxicity. The lignin-incorporated nanogel possessed antioxidant activity as it reduced active oxygen level, protecting the LO2 cells from apoptosis caused by oxidative stress. More importantly, *in vivo* studies demonstrated that the lignin-incorporated nanogels accelerated the healing of burn wounds in mice as proved by the increased expression of Ki67, one marker of cell proliferation. Present work demonstrates that lignin-incorporated nanogel could serve as an antioxidant wound-dressing material and facilitate the wound healing.

KEYWORDS

Lignin, Hydrogel, Gelation, Oxidation, Free Radicals, Wound Healing

INTRODUCTION

Wounds are defined as skin defects or ruptures caused by physical/thermal damage or underlying medical/physiological activity.[1-3] A large amount of oxygen free radicals is produced by the wounds[4] and this can increase the permeability of the cell capillary wall, leading to damage of vascular endothelial cells and wider cell necrosis and tissue dissolution.[5-7] Although most wounds heal gradually over time, the presence of external oxidative stimuli and bacterial infections

often impede wound healing.[4] Therefore, antioxidants that can block or delay the oxidation process by scavenging free radicals[8] are believed to be promising strategy for promoting wound recovery.

Lignin is a scavenger of oxygen free radical and is thought to be able stabilise the reactions initiated by oxygen radicals.[9, 10] Lignin contains a large amount of aromatic compounds.[11-14] It consists of up to three different phenylpropane monomers[15, 16] and contains a large amount of benzene rings and phenolic hydroxyl groups.[17-19] These aromatic moieties not only make lignin resistant to oxidation, but also enable lignin to be an ultraviolet protective agent as the aromatic moieties allow lignin to absorb ultraviolet radiation.[9, 20, 21] The antioxidant activities of lignin have been investigated by other research groups previously. Xue et al. demonstrated a response surface method to prepare a variety of organosolv lignin samples under different conditions[22] and evaluated their antioxidant properties. The results showed that lignin with smaller molecular weight and more phenolic hydroxyl groups had higher antioxidant activity. Xin et al. studied the antioxidant and antibacterial activities of lignin extracted from corn straw in alcohol production.[11] The extracted lignin showed high antioxidant activity as assessed by the hydrophilic oxygen radical absorbance capacity assay and modified Folin–Ciocalteu test.

Due to lignin's attractive antioxidant property, recent studies have begun to explore its potential application as antioxidant agent for healthcare.[23] Our group have designed and developed several lignin-based materials with excellent antioxidant properties and biocompatibility.[24-26] By using solvent-free ring-opening polymerization, Wang et al. synthesized copolymers composed of lignin and polycaprolactone (PCL), and combined these lignin-PCL polymers with pure PCL to make nanofiber scaffolds, which showed antioxidant activity.[27] Using the same method, Liang et al. prepared a PCL-grafted lignin (PCL-g-lignin),[28] in which lignin offers antioxidant activity while PCL tailors its mechanical properties. Then, nanofibers were fabricated with this PCL-lignin *via*

electrospinning, and both H_2O_2-stimulated human chondrocytes and an osteoarthritis rabbit model were used to demonstrate the remarkable antioxidant activity, tiny cytotoxicity, and splendid anti-inflammatory properties of the obtained nanofiber. Although lignin has started to be used as biomaterial, its applications in tissue engineering and biomedical fields are still limited, due to its not fully understood biocompatibility.[27, 29, 30]

For effective wound healing, a biocompatible carrier is needed to secure the lignin to the wound site. To this end, hydrogels are excellent candidates. Compared with traditional hemostatic materials such as pad and bandage, hydrogels exhibit high biocompatibility and similar physicochemical properties to natural tissues due to their high water content.[31] This feature also allows them to be non-adherent and cooling to the wound surface, thus promoting moist wound healing with marked reduction in pain.[2,32] Moreover, hydrogels are known for their ability to encapsulate a wide variety of molecules and nanoparticles.[33, 34] Thus, a hydrogel can be utilized as a reservoir to localize lignin to the wound site for effective antioxidant activity. As a type of hydrogel, nano-sized gels (nanogels) have been of great interest as nanocarriers in drug delivery systems.[35, 36] Thermo-responsive nanogels are particularly attractive because of their facile temperature controlled sol-gel transitions.[37] The thermo-responsive nanogels are supramolecular hydrogels formed *via* the self-assembly of amphiphilic copolymers,[38] and the gelation of the nanogel is achieved *via* micellization of the amphiphilic copolymers in aqueous solution followed by the aggregation of these micelles into a three-dimensional nanogel network.[39] They are in the sol phase at low temperatures and transit to the gel phase when the temperature is increased beyond the gelation temperature.[38] Therefore, thermo-responsive nanogels with the appropriate gelation temperature can be applied as liquid to the wound site and would gelate based on the shape of the wound, as they absorb physiological heat and transit to the gel phase. In addition, lignin can be

easily incorporated to the thermo-responsive nanogels in the sol phase, thus allowing facile production of lignin-incorporated nanogels.

Herein, we prepared lignin-incorporated nanogels and evaluated its application as antioxidant biomaterials to promote the wound healing and tissue regeneration. Lignin was extracted from coconut husks, and the antioxidant activity of the extracted lignin was evaluated *via* 1,1-diphenyl-2-pyridylmethylhydrazine test. The nanogel copolymer was synthesized by the polyaddition of macromonomer-diols (polyethylene glycol (PEG), polypropylene glycol (PPG), and polydimethylsiloxane-diol (PDMS-diol)) with hexamethylene diisocyanate (HMDI). Lignin was incorporated into the nanogel to produce lignin-incorporated nanogel composite (**Figure 1**). The micelle properties of the lignin-incorporated nanogel were studied, and dynamic rheological analysis of the nanogel was carried out. The biocompatibility of lignin-incorporated nanogel was assessed *in vitro* with LO2 cells *via* thiazolyl blue tetrazolium bromide (MTT) assay. Furthermore, the lignin-incorporated nanogel was implanted into mice wound models to evaluate its performance as an antioxidant wound dressing biomaterial. In summary, in present study a lignin-incorporated nanogel was prepared which functionally promoted wound healing, suggesting a novel strategy for wound care with the functional biomass nanogel.

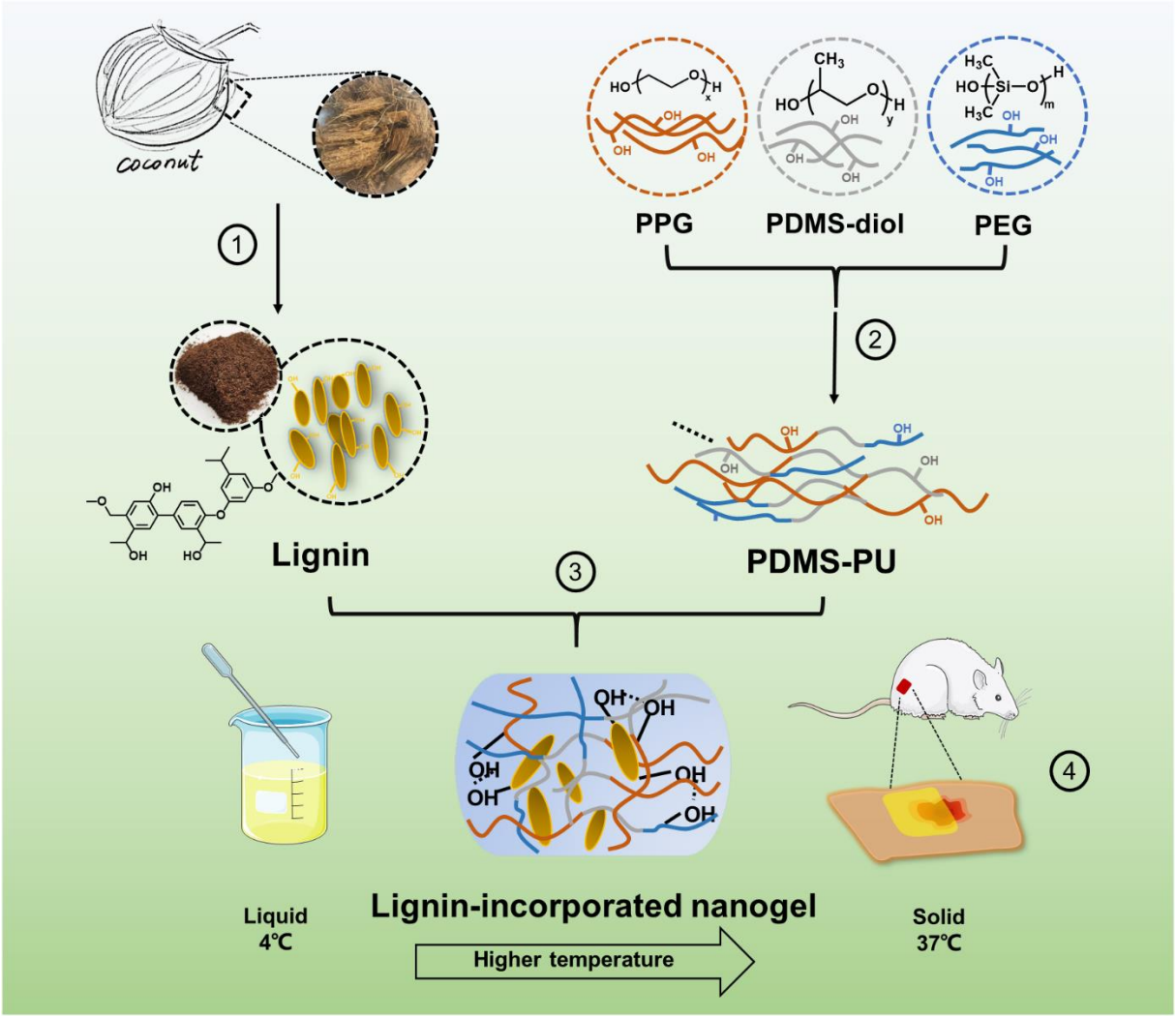

Figure 1. Schematic diagram of the preparation of lignin-incorporated nanogel for wound healing. ① Extraction of lignin from coconut husk; ② synthesis of thermo-responsive nanogel; ③ preparation of lignin-incorporated nanogel; and ④ application of the nanogel to treat wounds.

RESULTS AND DISCUSSION

Lignin is naturally abundant in wood and grass, but ways to extract lignin are still debatable. Currently, the widely adopted methods to extract lignin include soda process,[40] kraft process,[41] and sulfte pulping.[42] In this work, we used the organic solvent extraction method to extract lignin from coconut husks. This extraction method used less toxic chemical reagents and the extracted

lignin had a high purity. An organosolv lignin was obtained. The molecular weights (M_W) of lignin was determined to be 6.1 kDa by gel permeation chromatography (GPC) and the polymer dispersity (Đ) is 5.91. Two characteristic chemical displacement shifts of lignin, 3.85 ppm and 6.85 ppm, were observed in ^{1}H NMR spectrum, which correspondence to the methoxy protons and the protons of phenyl rings, respectively (**Figure 2A**). As shown in the ^{31}P NMR spectrum of lignin (**Figure 2B**), the peaks of aliphatic OH groups, syringyl OH groups, guaiacyl OH groups, and p-hydroxyphenyl OH groups of the lignin located at 150-145 ppm, 144-141 ppm, 141-138.5 ppm and 138.5-136 ppm, respectively. These results match the three basic structures of lignin. By calculation, aliphatic OH groups are of 5.727 mmol·g^{-1}, syringyl OH groups are of 0.245 mmol·g^{-1}, guaiacyl OH groups are of 1.368 mmol·g^{-1}, and p-hydroxyphenyl groups are of 1.2 mmol·g^{-1}. The total OH groups is thus 8.54 mmol g^{-1}. **Figure 2C** shows the FT-IR spectrum of the lignin. The broad peak at 3437 cm^{-1} is assigned to OH stretching. The strong bands at 1634 cm^{-1}, 1512 cm^{-1} and 1463 cm^{-1} are assigned to the conjugated carbonyl stretching, asymmetric aryl ring stretching, and asymmetric C-H deformation, respectively. The bands at 1198 cm^{-1} and 1114 cm^{-1} are assigned to the C-O-C stretching of ether bond. The functional band distribution of the sample is in accordance with known lignin.

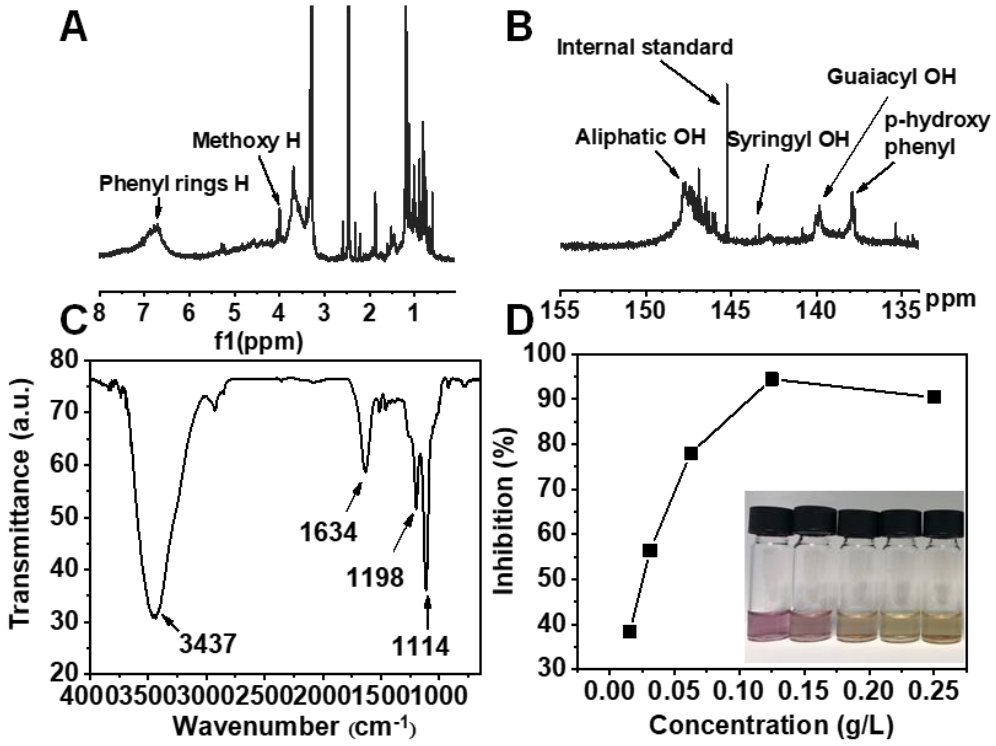

Figure 2. Characterization of lignin. (A) ^{1}H NMR spectrum of lignin. (B) ^{31}P NMR spectrum of lignin. (C) FT-IR spectrum of lignin. (D) Free radical scavenging capacity of lignin (inset: photos of different concentrations of lignin reacting with DPH).

It is known that phenol hydroxyl has strong reducing ability and lignin possesses three typical phenylpropane structures, which are the p-hydroxylphenyl, syringl, and guaiacyl units.[9] These endow lignin with strong antioxidant property, which is quantified *via* DPPH free radical scavenging test. **Figure 2D** shows the antioxidant activity of the extracted lignin. As the concentration of lignin increases, its free radical scavenging capacity also increases, and the overall trend is increasing. The free radical scavenging capacity of lignin exceeds 90% when the lignin concentration is greater than 0.2 $g \cdot L^{-1}$. Therefore, the IC_{50} (the half maximal inhibitory concentration) of the lignin was calculated as 25.7 ppm. In comparison, the IC_{50} of common antioxidants such as vitamin C, (+)-catechin hydrate, and Trolox are 15 ppm, 0.43 ppm, and 2.75

ppm respectively. These molecules are classified as strong antioxidants and have been explored as antioxidative agents to combat against cellular oxidative stress for biomedical applications.

The nanogel of poly (PEG/PPG/PDMS urethane) (PDMS-PU) random multi-block amphiphilic copolymer was synthesized from the polyaddition reaction of the respective macromonomer-diols with hexamethylene diisocyanate (HMDI) in the catalysis of dibutyltin-dilaurate (DBT) in anhydrous toluene. The scheme for synthesis of this polyurethane copolymer is shown in **Figure S1**. The molecular weight (Mw) of the copolymer was measured *via* GPC to be 49.6 kDa with Đ of 1.47. **Figure S2** shows the ^{1}H NMR spectrum of copolymer and the specific peaks from each component were present. In detail, the proton peak of PEG was observed at 3.52 ppm, while the proton peaks of PPG were observed at 3.5-3.3 ppm & 1.1 ppm, and the proton peaks of PDMS were observed at 0.06 ppm. As shown in the FT-IR spectrum of the poly (PEG/PPG/PDMS urethane) copolymer (**Figure S3**), all PDMS characteristic peaks at 1702, 2917 and 3414 cm^{-1} were present in final polyurethane spectra and the characteristic peaks of PEG and PPG were also observed at 1106, 947 and 843 cm^{-1}. This further confirms the composition and successful synthesis of poly (PEG/PPG/PDMS urethane) copolymer. The introduction of PDMS in the copolymer increased the hydrophobicity of the nanogel, which reduced the possibility of the nanogel adhering to the wound site, avoiding pain and hurt during pad changing or removing process.

Afterward, a series of lignin-incorporated nanogels were prepared by incorporating lignin into PDMS-PU nanogel, namely PPL1, PPL2, PPL3, PPL3, PPL4, PPL5 (**Table 1**). The critical micelle concentration (CMC) of the PDMS-PU copolymer was determined at 25°C using 1,6-diphenyl-1,3,5-hexatriene (DPH). DPH can be employed to determine CMC as its absorption coefficient increases much more significantly in a hydrophobic environment than in an aqueous environment.

The characteristic absorption wavelengths of DPH were at 344, 358, and 378 nm and the intensity of absorption increased as the polymer concentration increased (**Figure S4**). The concentration at which the absorbance of DPH increases significantly corresponds to the CMC. Micelles are first formed at the CMC and DPH are preferentially encapsulated into the hydrophobic core of the micelles, therefore resulting in the sudden increase in absorbance. The CMC was obtained by subtracting the absorbance at 400 nm from the absorbance at 378 nm and plotting the values against log (concentration). Two best fit lines are drawn in the unimer and micellar regions, and their intersection of the best fit lines is the CMC (**Figure 3A**). The CMC of different samples are shown in **Table 1** and it is found that higher lignin composition results in increased CMC; CMC increased from 4.23×10^{-4} to 10.2×10^{-4} g·mL^{-1} (**Table 1**) as lignin content increased from 0.05% to 1%.

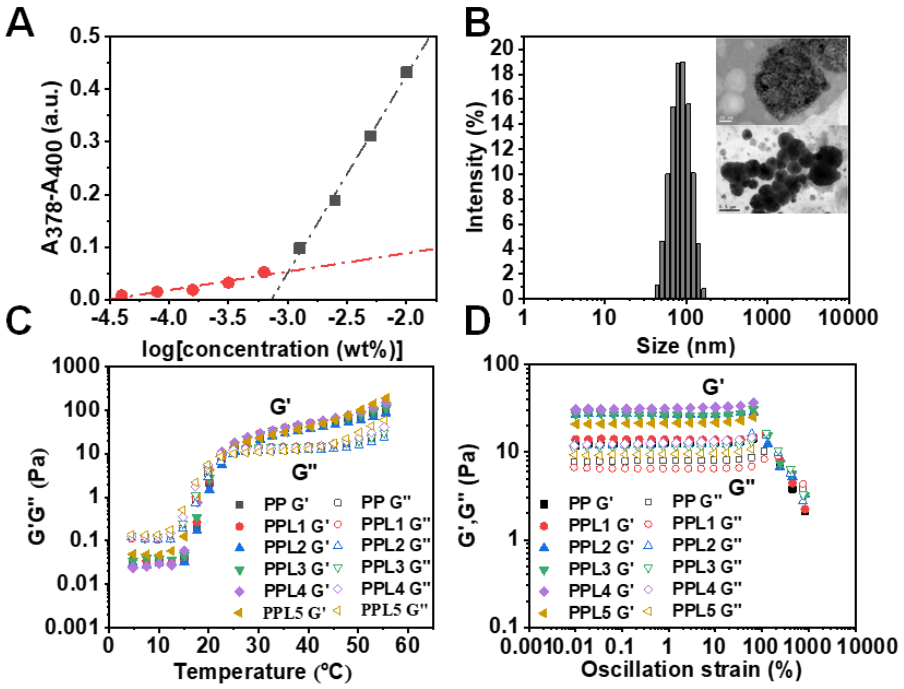

Figure 3. Characterization of lignin-incorporated nanogels. (A) Determination of the CMC of lignin-incorporated nanogels by extrapolating the difference in absorbance at 378 nm and 400 nm. (B) Particle size of lignin-incorporated nanogels (inset: TEM images of lignin-incorporated

nanogel). (C) Dynamic rheological analysis of aqueous solution of lignin-incorporated nanogels as a function of temperature. (D) Storage modulus (G') and loss modulus (G") as a function of strain amplitude for lignin-incorporated nanogels.

Figure 3B shows the size distribution of the lignin-incorporated nanogel micelles as determined by DLS. The micelles of the PDMS-PU nanogel are 67.89 nm and the polydispersity index (PDI) is 0.22. The addition of various amounts of lignin to the nanogel micelles does not lead to significant changes in micelle sizes as the micelle sizes remain approximately 70 nm. The sizes and PDI of the nanogel micelles incorporated with varying amounts of lignin are shown in **Table 1**. Under the transmission electron microscope (TEM), it is observed that 1% (w/v%) lignin-incorporated nanogel had a micelle particle size of about 10-500 nm (**Figure 3B**) while the lignin nanoparticles themselves had a uniform particle size of ~100 nm. The addition of lignin did not affect the micellar shape and size and did not affect the gelation ability of the PDMS-PU nanogel. The PDMS-PU nanogel encapsulated and maintained the fine dispersion of the lignin particles such that the lignin nanoparticle size remained at 100 nm. Without the nanogel to maintain the dispersion of the lignin nanoparticles, these nanoparticles could form aggregates of sizes exceeding 250 nm and with PDI = 0.461 (**Table 1**).

Table 1. Particle size, PDI, CMC and zeta potential of lignin-incorporated nanogel micelles at different lignin concentration.

Sample	Polymer (%)	Lignin (%)	CMC ($x10^{-4}$ $g \cdot mL^{-1}$)	Size (nm)	PDI	Zeta potential (mV)
1	1	0	3.38	67.89	0.220	-7.63
2	0	0.5	/	270.8	0.461	-16.0
3	1	0.05	4.23	69.23	0.265	-6.89
4	1	0.1	4.61	74.43	0.256	-14.2
5	1	0.2	5.72	72.89	0.228	-21.2
6	1	0.5	6.31	74.89	0.215	-20.6
7	1	1	10.2	72.07	0.183	-21.9

The rheological properties and thermo-gelling behavior of the lignin-incorporated nanogel was measured using a temperature-controlled rheometer. As the temperature rose from 4 to 55°C, a crossover of the storage modulus (G′) and loss modulus (G″) was observed at 22°C (**Figure 3C** and **Table 2**), indicating a sol-gel transition at this temperature. At low temperature of 4-25°C, the lignin-incorporated nanogel was in liquid form, which was indicated by the higher G" compared to G'. When the temperature was above the gelation temperature, the lignin-incorporated nanogel transited to the gel phase and became a non-flowable physical gel with G′ exceeding G″. The addition of lignin to PDMS-PU only resulted in slight changes to the crossover temperature from 22.9℃ to 21.9℃ (**Table 2**), thus the incorporation of lignin does not reduce the thermo-gelation ability of the nanogel.

Further rheological investigations were carried out on the lignin-incorporated nanogels by conducting oscillation amplitude sweep measurements at 37℃ (**Figure 3D**). It is observed that the modulus of PDMS-PU nanogel (PP) is strain independent initially at small oscillation amplitudes, but reaches a yield point at 23% strain before collapsing at higher oscillation amplitudes. The

incorporation of lignin into the nanogel improves the yield strain of the nanogel. As lignin content increases from 2 mg to 40 mg (PPL1 to PPL5, **Table 2**), the lignin-incorporated nanogel yield strain increases from 28% to 42% before collapsing as the strain amplitude increases further. This suggests that the lignin nanoparticles encapsulated in the nanogel improves the mechanical properties of the nanogel. Furthermore, it is observed that the viscoelastic properties of the lignin-incorporated nanogels are recovered once the external strain is removed. The rigid lignin macromolecules may be able to form entanglements and physical crosslinks with the flexible PDMS-PU nanogel copolymer leading to enhanced mechanical properties of the nanogel. The storage and loss moduli of the nanogel samples increase as lignin content increases such that PPL5 with the highest lignin content has the highest moduli (G' = 34 Pa and G" = 14 Pa). Due to the facile sol-gel phase transition of the nanogel, the nanogel in sol phase can accommodate the shape of the wound well before gelation and localizing the antioxidant lignin to the wound and promote healing.[4] Moreover, the softness of the nanogel improves patient comfort and reduce pain to the patient.[43]

Table 2. Dynamic rheological analysis of lignin-incorporated nanogel.

Sample	Polymer (mg)	Lignin (mg)	Water (mL)	G' (Pa)		G" (Pa)		Crossover Temperature (°C)
				25 °C	37 °C	25°C	37°C	
PP	600	0	10	14.8	41.2	11.5	13.6	22.9
PPL1	600	2	10	15.8	43.9	12.0	14.5	22.9
PPL2	600	4	10	11.2	32.5	9.5	11.8	23.9
PPL3	600	8	10	15.7	41.9	11.9	14.1	22.9
PPL4	600	20	10	17.9	43.4	12.0	13.3	21.9
PPL5	600	40	10	14.2	34.8	9.8	11.6	21.9

LO2 cells (human hepatocyte cells) were used to assess the biological toxicity of lignin. The LO2 cell line is considered an ideal cell model to test drug toxicity and protection in organisms.[44] LO2 cells are co-cultured with different concentrations of lignin (0.001-5%) for 24 hours and cell viability after treatment is quantified *via* MTT assay (**Figure 4A)**. Lignin demonstrates high biocompatibility at all tested concentrations as cell viability remained above 90% for all tested lignin concentrations. This suggests that lignin-incorporated nanogel can be regarded as a non-cytotoxic biomaterial in accordance to ISO 10 993.[45] The biocompatibility of lignin has also been evaluated in literature. Oihana et al. extracted lignin from hazelnut and walnut shells and evaluated its cytotoxicity *via* MTT assay on mouse fibroblast 3T3 cell line. Their results suggest good biocompatibility of lignin as cell viability is assessed to be 85% when cultured with 0.5% lignin.[46] Xu et al. synthesized polysiloxane-based polyurethane/lignin elastomers and found that the incorporation of 1wt% lignin to the elastomers improved the cell viability of HeLa cells to 65.2% as quantified by MTT assay.[47] Therefore, comparing our results to that in literature suggests that our organic solvent extracted lignin from coconut husks also possesses good biocompatibility and thus suitable for wound treatment applications.

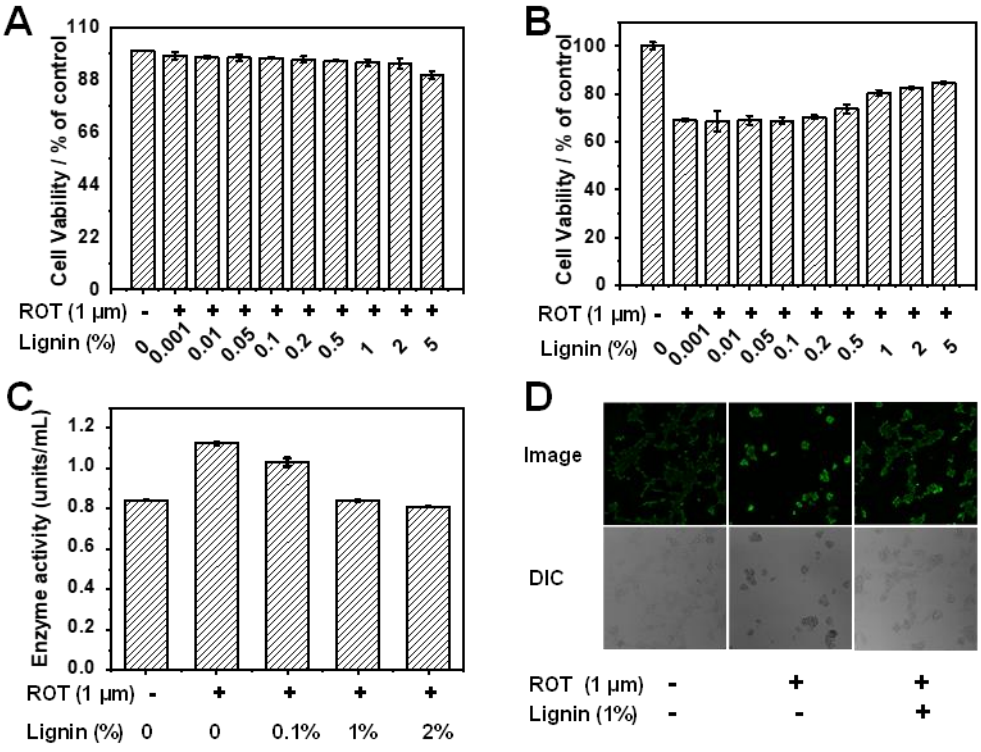

Figure 4. *In vitro* assessment of lignin-incorporated nanogel. (A) Toxicity of lignin-incorporated nanogel to LO2 cells at different concentrations. (B) Protective effect of different concentrations of lignin-incorporated nanogel on rotenone (ROT)-induced oxidative stress model of LO2 cells. (C) Catalase activity test of lignin-incorporated nanogel. (D) The change of intracellular reactive oxygen species (ROS) level was assessed by using the reactive oxygen species fluorescence assay kit (DCFH-DA) in ROT-induced oxidative stress model of LO2 cells with and without pre-incubation with lignin.

In addition, the antioxidant activity of lignin is assessed using the Rotenone (ROT) induced oxidative stress cell model and the results are shown in **Figure 4B**. Compared with the blank group (DMSO), the group pretreated with 1 μM ROT for 24 h showed a survival rate of 64%. The administration of different concentrations of lignin (0.001%-5%) prior to the 1 μM ROT exposure resulted in dose-dependent improved survival rates with a maximum survival rate of 83%. This

result suggested that lignin is able to protect cells against oxidative stress associated cytotoxicity due to the ROT treatment. Catalase is another antioxidant defense enzyme produced by cells to scavenge reactive oxygen species (ROS).[48] In response to a highly oxidative environment, cells increase production of catalase to protect themselves against oxidative stress. We further evaluated the antioxidant capacity of lignin by assessing the amount of catalase produced in cells incubated with varying amounts of lignin prior to ROT exposure. The antioxidant activity of lignin is expected to offer oxidative protection to cells and thus cells would respond by producing less catalase. As shown in **Figure 4C**, a significant increase in catalase level was observed in the group with 1 μM ROT administration as compared with the DMSO-only group, indicating that the excessive ROS caused by ROT led to increased expression of catalase in LO2 cells. However, the addition of lignin (0.01%, 0.1% and 2%) resulted in significantly reduced catalase production in cells.

In addition to catalase production in cells, the intracellular ROS level is also assessed as this indicates the extent of oxidative damage induced in cells. The DCFH-DA assay was used to assess the ROS level and it was found that exposure of LO2 cells to 1 μM ROT led to a significant increase in green fluorescent signal, suggesting significant oxidative cell damage compared to the control (**Figure 4D).** However, pre-treatment of the LO2 cells with lignin prior to ROT exposure led to significantly reduced DCF fluorescence signal, this suggests that lignin effectively reduced the level of intracellular ROS. This demonstrates lignin is an effective antioxidant possessing beneficial effects associated with regulation of cellular redox balance. Moreover, we believe that lignin, being a macromolecule antioxidant extracted from plants, is chemically more stable as compared to small-molecule antioxidants such as vitamin C, and thus we expect lignin to exert longer-lasting antioxidant effects on wounds.[14]

The performance of lignin-incorporated nanogel on promoting wound healing was evaluated by applying the lignin-incorporated nanogel on a mice burn model and assessing the macroscopic wound surface over time.[49] According to reports, ROS could hinder the wound healing, thus the application of antioxidant ROS scavengers such as lignin to the wound area is expected to accelerate the healing process.[50] The performance of lignin-incorporated nanogel at promoting wound recovery in mice burn wound model is compared to the performance of other antioxidants such as Vitamin C (V_C), Trolox, and (+)-catechin hydrate ((+) CE) applied to the wound (a photo showing how the nanogel was initially applied as a wound dressing is presented in **Figure S5**). As shown in **Figure 5** and **Figure 6**, the burn wound of the mice treated with lignin-incorporated nanogel completely healed by 25 days. In contrast, the mice of model group that received no antioxidant treatment exhibited a slower recovery rate. The rate of healing of the mice treated with lignin-incorporated nanogel was comparable to that of the mice treated with nanogels containing V_C and Trolox. This demonstrates that the lignin-incorporated nanogel possesses strong antioxidant activity and is highly effective at promoting wound recovery. However, when compared to the mice treated with (+) CE, it was found that the application of (+) CE allowed for the fastest rate of recovery.

The wound healing process was further investigated by conducting Ki67 staining and H&E staining on wound skin tissue sections. As shown in **Figure 7**, Ki67 protein increased in lignin-incorporated nanogel group (brown area increased) by Day 5, indicating that cell proliferation activity was higher and that the wound began to recover in a shorter period of time as compared to the model group with no antioxidant. This is similar to the results obtained from mice treated with (+) CE, as mice treated with (+) CE also exhibited higher Ki67 expression than the mice treated with no antioxidant by Day 5. It is found that the expression of Ki67 in the mice treated

with (+) CE and lignin-incorporated nanogel decreased by Day 15, indicating decreased cell proliferation activity which may be due to the good recovery already achieved in these two groups. In contrast, the Ki67 expression level in the mice of model group and Trolox group only began to increase after five days, suggesting a delayed recovery process as compared to the mice of (+) CE group and lignin-incorporated nanogel group. This result suggests that the lignin-incorporated nanogel is highly effective at promoting wound recovery.

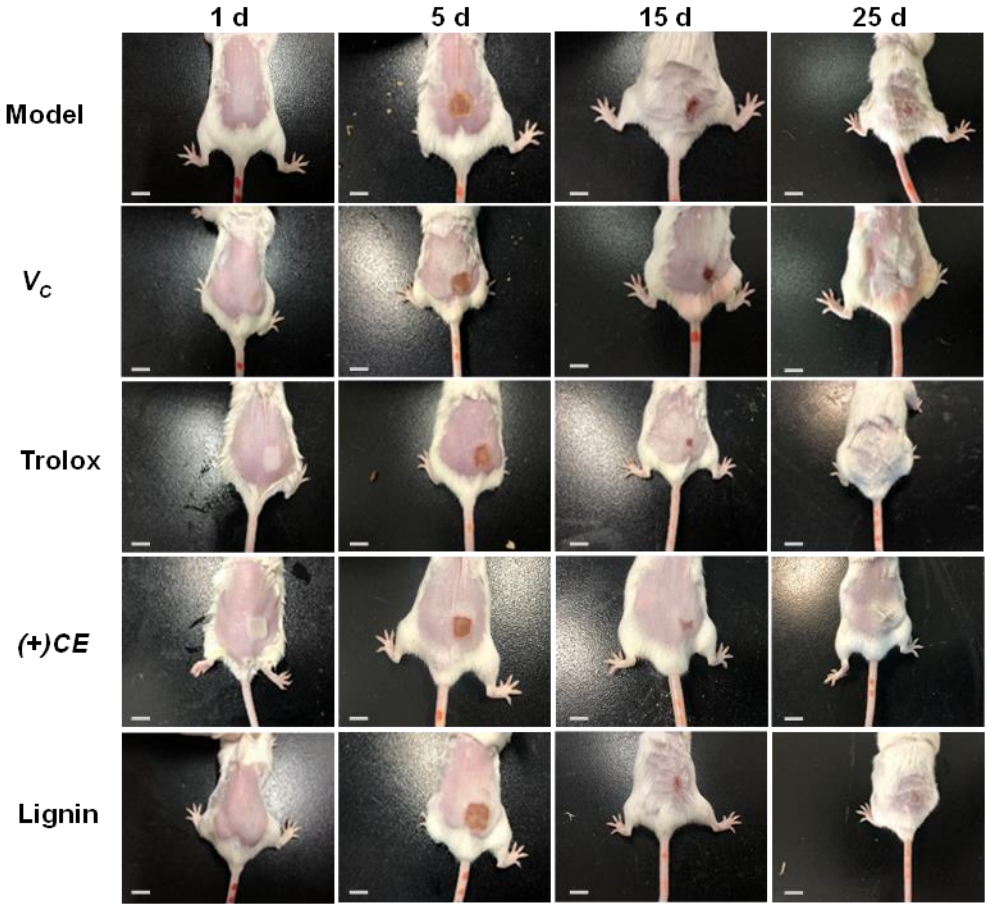

Figure 5. Images of skin wounds of the mice treated with nanogels containing V_C, Trolox, (+) CE, and lignin group on day 1, 5, 15, and 25, respectively (model group: mice treated with no antioxidant). Scale bar: 1 cm.

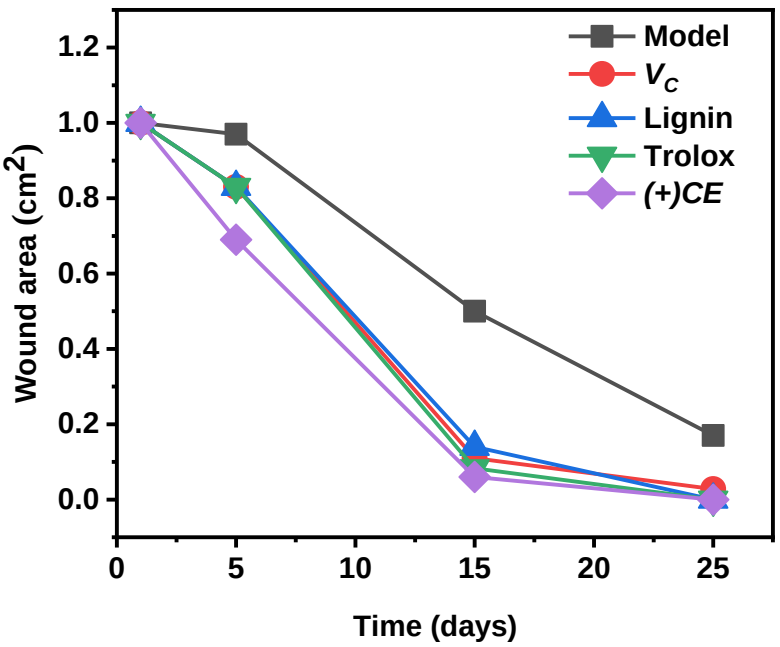

Figure 6. Statistics of the change in wound area. A graph showing the change in wound area over time on the mice treated with nanogels containing V_C, Trolox, (+) CE, and lignin (model group: mice treated with no antioxidant).

Results from the H&E staining (**Figure S6**) show that there were more inflammatory cells in the model group and fewer inflammatory cells in the mice treated with various antioxidants. In addition, regenerated hair follicles and epithelium were observed for the mice treated with Trolox, (+) CE, and lignin-incorporated nanogels. These results demonstrate that lignin-incorporated nanogel is highly effective at reducing wound inflammation and promoting wound tissue regeneration. Therefore, lignin-incorporated nanogel has high potential to be developed into an antioxidant wound dressing biomaterial.

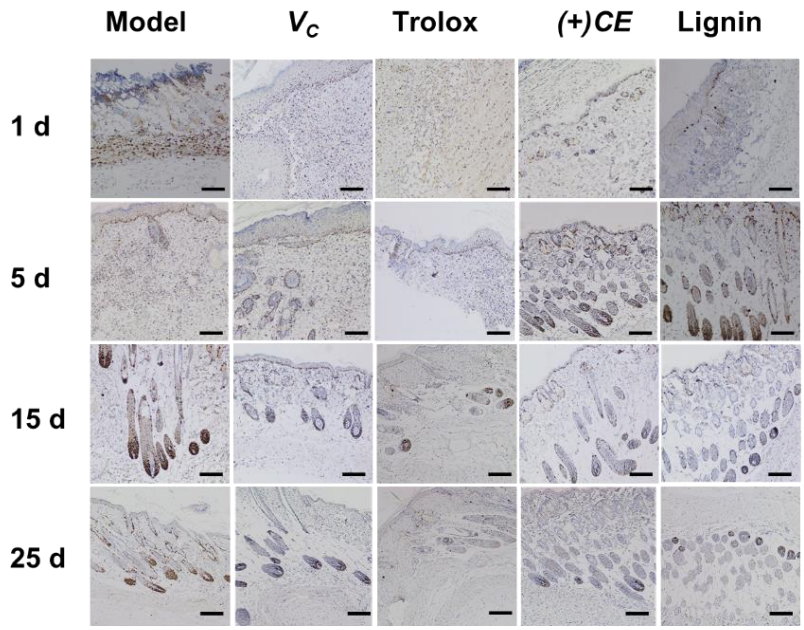

Figure 7. Ki67 stained sections of the mice granulation tissue. Images of model group, V_C group, Trolox group, (+) CE group and lignin-incorporated nanogel group on day 1, 5, 15, and 25, respectively. Scale bar: 200 μm.

CONCLUSIONS

In this study, antioxidant lignin was extracted from coconut husks and incorporated into poly (PEG/PPG/PDMS urethane) nanogel to obtain lignin-incorporated nanogel composites. The lignin-incorporated nanogel possesses both the antioxidant property of lignin and the nanogel ability of the PDMS-PU nanogel. It is able to scavenge the ROS at the wound site and also able to accommodate the shape of the wound, making it an excellent candidate biomaterial to promote wound recovery. *In vitro* assessment demonstrates that the lignin-incorporated nanogel had good biocompatibility and was non-cytotoxic, thus suggesting that lignin-incorporated nanogel is safe for skin application. The high biocompatibility of lignin-incorporated nanogel is essential such that it does not cause skin irritation when applied to the wound. Lignin-incorporated nanogel was assessed in mice burn wound models and was proved to accelerate wound recovery. This

demonstrates that lignin-incorporated nanogel has the potential to be developed into an effective antioxidant wound dressing biomaterial. Noteworthily, an added advantage of lignin is that it is highly abundant in nature and this would potentially allow for facile production of lignin-incorporated nanogels. Present study paves the way to obtain more comprehensive wound dressing materials by applying different bioactive molecules.

MATERIALS AND INSTRUMENTS

Materials. Coconut husk was dried at 110°C for 16 h before use. Unless otherwise stated, all chemicals were purchased from Sigma-Aldrich Chemicals and used as is. Human normal liver cells (LO2) were purchased from the American Type Culture Collection (ATCC). SPF mice were purchased from Qinglongshan Animal Breeding Field (Nanjing, China). All mice studies were performed following the appropriate guidelines (no. 20170201) and approved by the Institutional Animal Care and Use Committee at Nanjing Tech University (Nanjing, China).

Extraction and characterization of lignin. Solvent used for extraction was ethanol and deionized water (V:V=65:35) containing 1.5% H_2SO_4 as catalyst. 300 mL of the solvent was added to a 500 mL round bottom flask containing 15 g of coconut husk. The reaction mixture was stirred and heated under reflux at 70°C for 4 days before being filtered to give an extract, which was further adjusted to pH 7. The ethanol is removed by rotary evaporation and the obtained lignin was freeze-dried.

The molecular weight of lignin was analyzed by gel permeation chromatography (GPC) and the details were provided in our previous report.[27, 51] Thermogravimetric analysis (TGA) was performed using a thermogravimetric analyzer (Q500, TA Instruments, USA).[27] In a dynamic nitrogen atmosphere (flow rate = 60 $mL \cdot min^{-1}$), the samples were heated from room temperature

to 700°C at 20°C/min. The transmittance FT-IR spectra were obtained on a spectrophotometer (FT-IR-Spectrum 2000, Perkin Elmer). Samples prepared in KBr pellet were analyzed from 4000 to 600 cm^{-1} at a resolution of 1 cm^{-1} and 64 scans. DSC thermal analysis was performed using DSC (Q100, TA Instruments, USA) equipped with automatic cooling accessory and calibrated with indium.[51] The particle size of lignin at different concentrations was measured on Malvern Dynamic light scattering (DLS) instrument with Zetasizer Software. The morphology and size of the particle were observed on a transmission electron microscope (TEM) (JEOL JEM-2100). The ^{1}H and ^{31}P NMR was carried out on a Bruker NMR spectrometer (400 MHz and 162 MHz).

Antioxidant activity of lignin was assessed by 1, 1-diphenyl-2-picryl hydrazine (DPPH) assay and repeated three times.[51] By measuring the drop of absorbance compared to that of control solution, the free radical inhibition rate was obtained, which was used to determine the anti-radical activity of lignin. The phosphorylation of lignin was carried out by using a reported method.[52, 53]

Synthesis and characterization of nanogel. Poly (PDMS/PEG/PPG urethane)s were synthesized from the polyaddition reaction of $EG(PDMS\text{-}OH)_2$, PEG, and PPG with hexamethylene diisocyanate (HMDI). The molar ratio of PEG and PPG was set as 2:1, and the feed ratio for $EG(PDMS\text{-}OH)_2$ was 2 wt%. The operation details refer to a previous work.[54, 55] The precipitate was then air dried overnight before being dissolved in 200 mL of isopropanol (IPA) at 50°C. Dialysis was done to further purify the copolymer where the polymer IPA solution was poured into a dialysis membrane tubing (3.5-5 KD) and fully immersed in DI water. DI water was replaced every 2 h for a duration of 2 days. The obtained polymer solution was collected into falcon tubes and freeze dried. The obtained polymer was characterized by NMR, FT-IR, TGA and DSC. Nanogels were prepared by dissolving the purified copolymer into DI water.

Preparation and characterization of lignin-incorporated nanogel. Lignin-incorporated nanogels were prepared *via* a one-step method as shown in Table 1. Certain amount of lignin was added into 6 mL of 6% nanogels to achieve final concentration of 0.05%, 0.1%, 0.2%, 0.5%, and 1%. The CMC of lignin thermal gel was determined by dye dissolution method.[54] The absorbance spectrum was recorded by Shimazu UV-2501 PC UV-VIS spectrophotometer (Kyoto, Japan) at 25℃ from 320-420 nm. The absorbance difference at 378 nm and 400 nm (A_{378} - A_{400}) was plotted against the log(concentration). The CMC value of copolymer was determined by extrapolating linear fitting of non-monomer system and micelle system. The transmittance of the lignin-incorporated nanogel from 200 nm to 600 nm was measured by Shimazu UV-2501 PC UV-VIS spectrophotometer (Kyoto, Japan). The particle size of lignin-incorporated nanogels with different lignin content was measured using Malvern Dynamic light scattering (DLS) instrument with Zetasizer Software. The rheological behaviors of the polyurethane nanogels were determined on a Discovery DHP-3 hybrid rheometer.[54, 55]

Cell culture and cytotoxicity activity assay. The cytotoxic assay of lignin was determined using an MTT assay (Beyotime Biotechnology) by using a reported procedure.[56]

Intracellular antioxidation experiments. Intracellular ROS level was measured using the oxidation sensitive fluorescent probes DCFH-DA by following a reported procedure.[57]

Intracellular catalase activity assay. LO2 cells were grown on 6-well plates with 1640 medium containing gradient concentrations of lignin (0.1-2%) and rotenone (1 μM) for 24 h.[58] The catalase analysis kit (Beyotime Biotechnology) was used to evaluate catalase activity of LO2 cell lysates. The absorbance at 520 nm was measured using the microplate reader (Synergy 2, BioTek Instruments Inc).[48] Finally, the catalase activity was calculated through the formula in the manual.

Mice burned skin model. The treatment effect of lignin-incorporated nanogels on wound healing was validated using a mouse burn wound model. 4-6 weeks old healthy male Balb/C SPF mice with a weight of 18-20 g were adopted. The mice were divided into six groups, namely normal, model, lignin-incorporated nanogel, V_C, Trolox, and (+)-catechin hydrate ((+) CE) (Each group contains 15 mice). After anesthetized with isoflurane, the fur on the back of mice was removed with hair removal cream. The mice were secured on a clean bench limbs stage. A wet tissue with a hollowed rectangular area was used to confine the burning area (1.0 cm × 1.0 cm). Absolute ethanol was dropped to the 1 cm^2 fur of mice and the rest area was covered with thick wet tissue. Ethanol was ignited to cause skin burning and after 10 seconds the fire was extinguished with wet tissue.[59, 60] The six groups of mice were subjected to different treatments for their burn wounds. The various antioxidants were all dissolved at 1% concentration in the nanogel and applied to the burn wounds but the model group of mice received blank nanogels with no antioxidants. Three mice of each group were sacrificed successively on the 1^{st}, 5^{th}, 10^{th}, 15^{th}, and 25^{th} day after burning. The wound skin tissues were collected and stained for H&E and Ki67. Changes in body weight of the mice and surface area of the wound were constantly monitored and photographed (representative pictures of mice in each group are taken at the same photography angle).

ASSOCIATED CONTENT

Supporting Information

Synthetic scheme of PDMS-PU. ^1H NMR and FT-IR spectra of PP, UV-Vis spectra of DPH with increasing concentration of lignin-incorporated nanogels in water at 25°C.

AUTHOR INFORMATION

Corresponding Author

Lin Li, Email: iamlli@njtech.edu.cn

Hai-Dong Yu, Email: iamhdyu@njtech.edu.cn

Dan Kai, Email: kaid@imre.a-star.edu.sg

Notes

The authors declare no competing financial interest.

ACKNOWLEDGMENTS

This work was financially supported by the National Natural Science Foundation of China (21675085, 81672508, 61601218, and 61505076), Jiangsu Provincial Foundation for Distinguished Young Scholars (BK20170041, BK20170042), Key University Science Research Project of Jiangsu Province (Grant 16KJA180004) and China-Sweden Joint Mobility Project (51661145021). The authors also gratefully acknowledge the financial support from AME IAF-PP Specialty Chemicals Programme (Grant No. A1786a0034) and CDA (Project No. CDA 202D800033), Agency for Science, Technology and Research (A*STAR).

REFERENCES

(1) Abdelrahman, T.; Newton, H., Wound Dressings: Principles and Practice. Surgery (Oxford) 2011, 29 (10), 491-495.

(2) Li, Z.; Zhou, F.; Li, Z.; Lin, S.; Chen, L.; Liu, L.; Chen, Y., Hydrogel Cross-Linked with Dynamic Covalent Bonding and Micellization for Promoting Burn Wound Healing. ACS Applied Materials & Interfaces 2018, 10 (30), 25194-25202.

(3) Xian, C.; Gu, Z.; Liu, G.; Wu, J., Whole Wheat Flour Coating with Antioxidant Property Accelerates Tissue Remodeling for Enhanced Wound Healing. Chinese Chemical Letters 2020, 31 (6), 1612-1615.

(4) Joshua, S. B.; Kerr, H. M.; Howard, N. E.S.; Gillian, M. E., Wound Healing Dressings and Drug Delivery Systems: A Review. Pharmaceutical Sciences 2008, 97 (8), 2892-923.

(5) Blokhina, O.; Virolainen, E.; Kurt, V., Antioxidants, Oxidative Damage and Oxygen Deprivation Stress: A Review. Annals of Botany 2003, 91 (5), 179-94.

(6) Homaeigohar, S.; Boccaccini, A. R., Antibacterial Biohybrid Nanofibers for Wound Dressings. Acta Biomaterialia 2020, 19 (11), 1234-1345.

(7) Fang, J.; Seki, T.; Maeda, H., Therapeutic Strategies by Modulating Oxygen Stress in Cancer and Inflammation. Advanced Drug Delivery Reviews 2009, 61 (4), 290-302.

(8) Blessy, B. M., Archana, T.; Suresh K. J., Free Radicals and Antioxidants: A Review. Pharmacy Research 2011, 4(12), 4340-4343.

(9) García, A.; González Alriols, M.; Spigno, G.; Labidi, J., Lignin as Natural Radical Scavenger. Effect of the Obtaining and Purification Processes on the Antioxidant Behaviour of Lignin. Biochemical Engineering Journal 2012, 67, 173-185.

(10) Wu, Y.; Qian, Y.; Lou, H.; Yang, D.; Qiu, X., Enhancing the Broad-Spectrum Adsorption of Lignin through Methoxyl Activation, Grafting Modification, and Reverse Self-Assembly. ACS Sustainable Chemistry & Engineering 2019, 7 (19), 15966-15973.

(11) Dong, X.; Dong, M.; Lu, Y.; Turley, A.; Jin, T.; Wu, C., Antimicrobial and Antioxidant Activities of Lignin from Residue of Corn Stover to Ethanol Production. Industrial Crops and Products 2011, 34 (3), 1629-1634.

(12) Larraneta, E.; Imizcoz, M.; Toh, J. X.; Irwin, N. J.; Ripolin, A.; Perminova, A.; Dominguez-Robles, J.; Rodriguez, A.; Donnelly, R. F., Synthesis and Characterization of Lignin Nanogels for Potential Applications as Drug Eluting Antimicrobial Coatings for Medical Materials. ACS Sustainable Chemistry & Engineering 2018, 6 (7), 9037-9046.

(13) Chen, S.; Wang, G.; Sui, W.; Parvez, A. M.; Dai, L.; Si, C., Novel Lignin-Based Phenolic Nanosphere Supported Palladium Nanoparticles with Highly Efficient Catalytic Performance and Good Reusability. Industrial Crops and Products 2020, 145, 112164.

(14) Zhou, Y.; Qian, Y.; Wang, J.; Qiu, X.; Zeng, H., Bioinspired Lignin-Polydopamine Nanocapsules with Strong Bioadhesion for Long-Acting and High-Performance Natural Sunscreens. Biomacromolecules 2020, 21 (8), 3231-3241.

(15) Spasojevic, D.; Zmejkoski, D.; Glamoclija, J.; Nikolic, M.; Sokovic, M.; Milosevic, V.; Jaric, I.; Stojanovic, M.; Marinkovic, E.; Barisani-Asenbauer, T.; Prodanovic, R.; Jovanovic, M.; Radotic, K., Lignin Model Compound in Alginate Nanogel: A Strong Antimicrobial Agent With High Potential in Wound Treatment. International Journal of Antimicrobial Agents 2016, 48 (6), 732-735.

(16) Qian, Y.; Zhou, Y.; Li, L.; Liu, W.; Yang, D.; Qiu, X., Facile Preparation of Active Lignin Capsules for Developing Self-healing and UV-blocking Polyurea Coatings. Progress in Organic Coatings 2020, 138, 105354.

(17) Qian, Y.; Zhong, X.; Li, Y.; Qiu, X., Fabrication of Uniform Lignin Colloidal Spheres for Developing Natural Broad-spectrum Sunscreens with High Sun Protection Factor. Industrial Crops and Products 2017, 101, 54-60.

(18) Dai, L.; Zhu, W.; Lu, J.; Kong, F.; Si, C.; Ni, Y., A Lignin-containing Cellulose Nanogel for Lignin Fractionation. Green Chemistry 2019, 21 (19), 5222-5230.

(19) Wang, J.; Qian, Y.; Li, L.; Qiu, X., Atomic Force Microscopy and Molecular Dynamics Simulations for Study of Lignin Solution Self-Assembly Mechanisms in Organic–Aqueous Solvent Mixtures. ChemSusChem 2020, 5(9), 269-291.

(20) Dai, L.; Ma, M.; Xu, J.; Si, C.; Wang, X.; Liu, Z.; Ni, Y., All-Lignin-Based Nanogel with Fast pH-Stimuli Responsiveness for Mechanical Switching and Actuation. Chemistry of Materials 2020, 32 (10), 4324-4330.

(21) Wu, Y.; Qian, Y.; Zhang, A.; Lou, H.; Yang, D.; Qiu, X., Light Color Dihydroxybenzophenone Grafted Lignin with High UVA/UVB Absorbance Ratio for Efficient and Safe Natural Sunscreen. Industrial & Engineering Chemistry Research 2020, 40, 7715-7755.

(22) Pan, X., John, F.; Katsunobu, E.; Neil G.; Jack, N.; Saddler, Organosolv Ethanol Lignin from Hybrid Poplar as A Radical Scavenger: Relationship between Lignin Structure, Extraction Conditions, and Antioxidant Activity. Agriculture Food Chemistry 2006, 54, 5806-5813.

(23) Chen, K.; Lei, L.; Qian, Y.; Yang, D.; Qiu, X., Development of Anti-Photo and Anti-Thermal High Internal Phase Emulsions Stabilized by Biomass Lignin as a Nutraceutical Delivery System. Food & Function 2019, 10 (1), 355-365.

(24) Kai, D.; Jiang, S.; Low, Z. W.; Loh, X. J., Engineering Highly Stretchable Lignin-Based Electrospun Nanofibers for Potential Biomedical Applications. Journal of Materials Chemistry B 2015, 3 (30), 6194-6204.

(25) Jiang, S.; Kai, D.; Dou, Q. Q.; Loh, X. J., Multi-Arm Carriers Composed of An Antioxidant Lignin Core and Poly(glycidyl methacrylate-co-Poly(ethylene glycol)methacrylate) Derivative Arms for Highly Efficient Gene Delivery. Journal of Materials Chemistry B 2015, 3 (34), 6897-6904.

(26) Kai, D.; Low, Z. W.; Liow, S. S.; Abdul Karim, A.; Ye, H.; Jin, G.; Li, K.; Loh, X. J., Development of Lignin Supramolecular Nanogels with Mechanically Responsive and Self-Healing Properties. ACS Sustainable Chemistry & Engineering 2015, 3 (9), 2160-2169.

(27) Wang, J.; Tian, L.; Luo, B.; Ramakrishna, S.; Kai, D.; Loh, X. J.; Yang, I. H.; Deen, G. R.; Mo, X., Engineering PCL/Lignin Nanofibers as An Antioxidant Scaffold for The Growth of Neuron and Schwann Cell. Colloids and Surfaces B: Biointerfaces 2018, 169, 356-365.

(28) Liang, R.; Zhao, J.; Li, B.; Cai, P.; Loh, X. J.; Xu, C.; Chen, P.; Kai, D.; Zheng, L., Implantable and Degradable Antioxidant Poly(ε-caprolactone)-Lignin Nanofiber Membrane for Effective Osteoarthritis Treatment. Biomaterials 2020, 230 (10), 601-613.

(29) Ten, E.; Ling, C.; Wang, Y.; Srivastava, A.; Dempere, L. A.; Vermerris, W., Lignin Nanotubes as Vehicles for Gene Delivery into Human Cells. Biomacromolecules 2014, 15 (1), 327-338.

(30) Dizhbite, T.; Telysheva, Galina, Jurkjane, Vilhelmina, Viesturs, Uldis, Characterization of The Radical Scavenging Activity of Lignins-Natural Antioxidants. Bioresource Technology 2004, 95 (3), 309-317.

(31) Saroia, J.; Yanen, W.; Wei, Q.; Zhang, K.; Lu, T.; Zhang, B., A review on Biocompatibility Nature of Nanogels with 3D Printing Techniques, Tissue Engineering Application and Its Future Prospective. Bio-Design and Manufacturing 2018, 1 (4), 265-279.

(32) Huang, J.; Chen, L.; Gu, Z.; Wu, J., Red Jujube-Incorporated Gelatin Methacryloyl (GelMA) Hydrogels with Anti-Oxidation and Immunoregulation Activity for Wound Healing. Journal of Biomedical Nanotechnology 2019, 15 (7), 1357-1370.

(33) Jiang, L.; Luo, Z.; Loh, X. J.; Wu, Y.-L.; Li, Z., PHA-Based Nanogel as A Controlled Zero-Order Chemotherapeutic Delivery System for the Effective Treatment of Melanoma. ACS Applied Bio Materials 2019, 2 (8), 3591-3600.

(34) Patel, M.; Lee, H. J.; Son, S.; Kim, H.; Kim, J.; Jeong, B., Iron Ion-Releasing Polypeptide Nanogel for Neuronal Differentiation of Mesenchymal Stem Cells. Biomacromolecules 2020, 21 (1), 143-151.

(35) Zhang, T.; Yang, R.; Yang, S.; Guan, J.; Zhang, D.; Ma, Y.; Liu, H., Research Progress of Self-Assembled Nanogel and Hybrid Hydrogel Systems Based on Pullulan Derivatives. Drug Delivery 2018, 25 (1), 278-292.

(36) Kabanov, A. V.; Vinogradov, S. V., Nanogels as Pharmaceutical Carriers: Finite Networks of Infinite Capabilities. Drug Delivery 2009, 48 (30), 5418-29.

(37) Eslahi, N.; Abdorahim, M.; Simchi, A., Smart Polymeric Nanogels for Cartilage Tissue Engineering: A Review on the Chemistry and Biological Functions. Biomacromolecules 2016, 17 (11), 3441-3463.

(38) Zarrintaj, P.; Mohammad R.; Hadavand; Behzad S.; Tomy J.; Mohammad R., Thermo-sensitive Polymers in Medicine: A review. European Polymer Journal 2019, 117, 402-423.

(39) Hoang Thi, T. T.; Sinh, L. H.; Huynh, D. P.; Nguyen, D. H.; Huynh, C., Self-Assemblable Polymer Smart-Blocks for Temperature-Induced Injectable Nanogel in Biomedical Applications. Frontiers in Chemistry 2020, 8 (19), 456-475.

(40) Ratanasumarn, N.; Chitprasert, P., Cosmetic Potential of Lignin extracts from Alkaline-treated Sugarcane Bagasse: Optimization of Extraction Conditions Using Response Surface Methodology. International Journal of Biological Macromolecules 2020, 153, 138-145.

(41) Tejado, A.; Peña, C.; Labidi, J.; Echeverria, J. M.; Mondragon, I., Physico-chemical Characterization of Lignins from Different Sources for Use in Phenol–formaldehyde Resin Synthesis. Bioresource Technology 2007, 98 (8), 1655-1663.

(42) Marques, A. P.; Evtuguin, D. V.; Magina, S.; Amado, F. M. L.; Prates, A., Structure of Lignosulphonates from Acidic Magnesium-Based Sulphite Pulping of Eucalyptus globulus. Journal of Wood Chemistry and Technology 2009, 29 (4), 337-357.

(43) Wichterle, O.; LÍM, D., Hydrophilic Gels for Biological Use. Nature 1960, 185 (4706), 117-118.

(44) Shao, Y.; Chen, Z.; Wu, L., Oxidative Stress Effects of Soluble Sulfide on Human Hepatocyte Cell Line LO2. International Journal of Environmental Research and Public Health 2019, 16 (9), 1662-1671.

(45) Musilova, L.; Mracek, A.; Kovalcik, A.; Smolka, P.; Minarik, A.; Humpolicek, P.; Vicha, R.; Ponizil, P., Hyaluronan Nanogels Modified by Glycinated Kraft Lignin: Morphology, swelling, viscoelastic properties and biocompatibility. Carbohydrate Polymers 2018, 181 (9), 394-403.

(46) Gordobil, O.; Olaizola, P.; Banales, J. M.; Labidi, J., Lignins from Agroindustrial by-Products as Natural Ingredients for Cosmetics: Chemical Structure and In Vitro Sunscreen and Cytotoxic Activities. Molecules 2020, 25 (5), 1131-1147.

(47) Xu, C.; Chen, G.; Tan, Z.; Hu, Z.; Qu, Z.; Zhang, Q.; Lu, M.; Wu, Kun, L.; Lu, M.; Liang, L., Evaluation of Cytotoxicity in Vitro and Properties of Polysiloxane-Based Polyurethane/Lignin Elastomers. Reactive and Functional Polymers 2020, 149, 1381-5148.

(48) He, Z.; Sun, X.; Mei, G.; Yu, S.; Li, N., Nonclassical Secretion of Human Catalase on the Surface of CHO Cells is More Efficient than Classical Secretion. Cell Biology International 2008, 32 (4), 367-373.

(49) Nooshabadi, V. T.; Khanmohamadi, M.; Valipour, E.; Mahdipour, S.; Salati, A.; Malekshahi, Z. V.; Shafei, S.; Amini, E.; Farzamfar, S.; Ai, J., Impact of Exosome Loaded Chitosan Nanogel in Wound Repair and Layered Dermal Reconstitution in Mice Animal Model. Journal of Biomedical Materials Research A 2020, (21), 5423-5436.

(50) He, J.; Liang, Y.; Shi, M.; Guo, B., Anti-oxidant Electroactive and Antibacterial Nanofibrous Wound Dressings Based on Poly(ε-caprolactone)/Quaternized Chitosan-Graft-

Polyaniline for Full-thickness Skin Wound Healing. Chemical Engineering Journal 2020, 385 (10), 123-464.

(51) Kai, D.; Zhang, K.; Jiang, L.; Wong, H. Z.; Li Z.; Zhang, Z.; Loh, X. J., Sustainable and Antioxidant Lignin-Polyester Copolymers and Nanofibers for Potential Healthcare Applications. ACS Sustainable Chemistry & Engineering 2017, 10, 178-187.

(52) Loh, X. J.; Gan, H. X.; Wang, H.; Tan, S. J. E.; Neoh, K. Y.; Jean Tan, S. S.; Diong, H. F.; Kim, J. J.; Sharon Lee, W. L.; Fang, X.; Cally, O.; Yap, S. S.; Liong, K. P.; Chan, K. H., New Thermogelling Poly(ether carbonate urethane)s Based on Pluronics F127 and Poly(polytetrahydrofuran carbonate). Journal of Applied Polymer Science 2014, 131 (5), 1941-1956.

(53) Nam Nguyen, V. P.; Kuo, N.; Loh, X. J., New Biocompatible Thermogelling Copolymers Containing Ethylene-Butylene Segments Exhibiting Very Low Gelation Concentrations. Soft Matter 2011, 7 (5), 2150-2159.

(54) Chan, B. Q. Y.; Cheng, H.; Liow, S. S.; Dou, Q.; Wu, Y. L.; Loh, X. J.; Li, Z., Poly(carbonate urethane)-Based Thermogels with Enhanced Drug Release Efficacy for Chemotherapeutic Applications. Polymers (Basel) 2018, 10 (1).

(55) Jiang, L.; Luo, Z.; Loh, X. J.; Wu, Y.-L.; Li, Z., PHA-Based Thermogel as a Controlled Zero-Order Chemotherapeutic Delivery System for the Effective Treatment of Melanoma. ACS Applied Bio Materials 2019, 2 (8), 3591-3600.

(56) Weng, M.; Yang, X.; Ni, Y.; Xu, C.; Zhang, H.; Shao, J.; Shi, N.; Zhang, C.; Wu, Q.; Li, L.; Huang, W., Deep-red Fluorogenic Probe for Rapid Detection of Nitric Oxide in Parkinson's Disease Models. Sensors and Actuators B: Chemical 2019, 283, 769-775.

(57) Ding, Y.; Kong, D.; Zhou, T.; Yang, N.-d.; Xin, C.; Xu, J.; Wang, Q.; Zhang, H.; Wu, Q.; Lu, X.; Lim, K.; Ma, B.; Zhang, C.; Li, L.; Huang, W., α-Arbutin Protects Against Parkinson's Disease-Associated Mitochondrial Dysfunction In Vitro and In Vivo. NeuroMolecular Medicine 2020, 22 (1), 56-67.

(58) Wang, J.; Zhang, J.; Chen, X.; Yang, Y.; Wang, F.; Li, W.; Awuti, M.; Sun, Y.; Lian, C.; Li, Z.; Wang, M.; Xu, J.-Y.; Jin, C.; Tian, H.; Gao, F.; Zhang, J.; Sinha, D.; Lu, L.; Xu, G.-T., MiR-365 Promotes Diabetic Retinopathy Through Inhibiting Timp3 and Increasing Oxidative Stress. Experimental Eye Research 2018, 168, 89-99.

(59) Ju, X.; M. S.; Zhao, H.; Yao, W.; Wei, M.; Establishment of a new rat burn model with paste solid alcohol burning method. Journal of Shenyang Pharmaceutical University 2008, 2, 134.

(60) Calum, H.; Høiby, N.; Moser, C., Mouse Model of Burn Wound and Infection: Thermal (Hot Air) Lesion-Induced Immunosuppression. Current Protocols in Mouse Biology 2017, 7 (2), 77-87.

GRAPHICAL ABSTRACT